FMDB *Transactions on Sustainable Environmental Sciences*

Sensitivity Analysis of Pressurized Water Transmission Pipelines: A Case Study of the Al-Hashimiyah Water Treatment System

Hayder Mohammed Kadhim[1], Mohammed S. Shamkhi[2], Ahmed Samir Naje[3,*]

[1,3]Department of Water Resources Engineering Management, College of Engineering, Al-Qasim Green University, Al-Qasim, Babylon, Iraq.
[2]Department of Structures and Water Resources, Faculty of Engineering, University of Kufa, Kufa, Najaf Governorate, Iraq.
[2]College of Engineering, University of Warith Al-Anbiyaa, Karbala Governorate, Iraq.
haidermohammed@wrec.uoqasim.edu.iq[1], yhjk6621@gmail.com[2], ahmednamesamir@gmail.com[3]

Abstract: The steady-state and transient flow behaviours of the Al-Hashimiyah Water Treatment pipeline system are examined in this hydraulic evaluation. The steady-state analysis showed a flow velocity of 5.66 m/s, a Reynolds number of 1.18×10^6, and a Darcy-Weisbach friction factor of 0.008. Total head losses, including friction and minor losses, were within the 70 m pressure head limit. A robust hybrid numerical model that merges the Method of Characteristics (MOC) and Method of Integration (MOI) accurately simulates pressure surges induced by unexpected valve closures and pump failures. In simulations, surge pressures reached 205.13 m at 0.347 m^3/s, exceeding operational safety requirements, whereas at 0.111 m^3/s they remained below 65.56 m. Pump power interruptions caused large pressure dips and negative pressures, leading to vapour pressure violations and increased cavitation risk. Researchers designed and simulated a surge tank with a diameter of 12 m and a height of 15 m, with an effective volume of 1,700 m^3, to mitigate transient impacts. The surge tank 70 m downstream of the initial pumping station lowered peak surge pressures by 24.6%. Sensitivity analyses showed that key hydraulic parameters affected the transient response: increasing the pipe diameter from 0.20 m to 0.35 m reduced surge pressure from 191.21 m to 122.32 m, and increasing the friction factor from 0.003 to 0.012 reduced surge pressure from 187.40 m to 149.80 m.

Keywords: Transient Flow; Water Hammer; Surge Tank; Pipeline System; Sensitivity Analysis; Water Transmission Systems; Hydraulic Evaluation; Hydraulic Engineering; Water Treatment.

Received on: 22/12/2024, **Revised on:** 25/02/2025, **Accepted on:** 19/05/2025, **Published on:** 16/12/2025

Journal Homepage: https://www.fmdbpub.com/user/journals/details/FTSESS

DOI: https://doi.org/10.69888/FTSESS.2025.000556

Cite as: H. M. Kadhim, M. S. Shamkhi, and A. S. Naje, "Sensitivity Analysis of Pressurized Water Transmission Pipelines: A Case Study of the Al-Hashimiyah Water Treatment System," *FMDB Transactions on Sustainable Environmental Sciences*, vol. 2, no. 4, pp. 210–226, 2025.

1. Introduction

The Water hammer is a transient hydraulic phenomenon characterised by rapid, sometimes extreme, pressure surges in pressurised pipeline systems, typically initiated by sudden changes in flow conditions, such as abrupt valve closures or pump failures [14]. These unsteady events pose significant risks to water infrastructure, often leading to pipe fatigue, structural damage, or operational disruptions, especially in extensive water transmission networks [28]; [32]. With the continued

*Corresponding author.

expansion of urban areas and rising water demand, addressing the adverse effects of water hammer has become a priority in hydraulic engineering [34]. Over recent decades, numerous studies have investigated the factors influencing transient flow behaviour, including pipe diameter, wall elasticity, internal friction, and boundary conditions [6]; [36]. Both experimental and numerical approaches have been employed to simulate such behaviours, with the Method of Characteristics (MOC) emerging as a widely accepted technique for modelling wave propagation during transients [33]. More recent advances involve coupling MOC with the Method of Implicit (MOI), which enhances numerical stability and is better suited for complex systems [10]. Studies by Qian et al. [39], Schulz et al. [5], and Sedlar and Abrahámek [24] have highlighted the effectiveness of these methods in capturing intricate interactions such as air entrainment and pump stoppages.

Abdulameer et al. [13] emphasised integrating surge mitigation components, such as air chambers and surge tanks, with MOC-based simulations to reduce transient-related failures in water supply systems. Furthermore, material properties significantly influence water hammer responses. Pipelines made of more flexible materials, such as polypropylene or uPVC, tend to exhibit lower pressure spikes due to their greater capacity for energy absorption [22]. Supporting this, Knapp et al. [11] and Liang et al. [8] used finite element modelling (FEM) and laboratory validation to examine strain and fatigue under transient loads, confirming the reliability of their models with minimal error margins. Additionally, frequency-dependent hydraulic resistance models proposed by Lupa et al. [29] and Urbanowicz et al. [12] have provided more accurate predictions for systems with low water hammer numbers [35]. Despite the growing body of international research, studies tailored to real-world pipeline systems in the Middle East, particularly Iraq, remain limited. Iraq's ageing water infrastructure is under increasing strain from rapid urbanisation and inconsistent operational practices [23]. The Al-Hashimiyah Water Treatment Plant, a key facility in the Babylon Governorate, delivers potable water to several districts via a complex, lengthy transmission system. Given the plant's operational variability and extensive pipeline length, it is particularly vulnerable to transient events, which may compromise service delivery and structural reliability [18]; [20].

To date, no comprehensive analysis has applied a combined MOC-MOI framework to model transient behaviour in this specific context, nor has any study examined the sensitivity of such a system to critical design and operational parameters, such as pipe diameter, discharge rate, or friction factor. This study seeks to address this gap by developing a MATLAB numerical model that integrates MOC and MOI techniques to simulate unsteady flow in the Al-Hashimiyah pipeline. Drawing on methodologies used by Negharchi and Shafaghat [30], Arefi et al. [21], and Meniconi et al. [31], the research incorporates a detailed sensitivity analysis to identify the most influential parameters and assess potential mitigation strategies, such as pressure relief mechanisms and valve operation optimisation. While existing research has yielded valuable insights under controlled or simplified conditions, much of it lacks direct applicability to field-scale systems experiencing fluctuating demands and uncertain boundary conditions. The current study advances the field by: (1) Identifying and quantifying the sensitivity of transient pressure responses to key hydraulic parameters; (2) Constructing a robust coupled MOC-MOI model tailored to the Al-Hashimiyah system; (3) Evaluating transient risks through parameter variation; (5) Recommending system-specific mitigation measures; and (6) Providing design insights aimed at enhancing the reliability, efficiency, and resilience of Iraq's water infrastructure. This investigation not only contributes to the global understanding of transient hydraulic behaviour in large-scale systems but also delivers regionally relevant strategies to support sustainable and safe water supply operations in Iraq.

2. Study Area and Methodology

2.1. Description of Selected Case Study

The focus of this study is the Al-Hashimiyah Water Treatment Plant, located in the southern region of Babylon Governorate, Iraq, at coordinates 32°22'42"N and 44°39'25" E, as illustrated in Figure 1. This facility represents a critical component of the region's water infrastructure, with a treatment capacity of 6,000 m^3/h, supplying clean water to over 250,000 residents across the districts of Al-Hashimiyah, Al-Qasim, Al-Tali'ah, Al-Shomali, and surrounding rural areas. As mentioned by Salmasi [18], the plant is organised into six major operational units: (1) Low Pumping Unit, (2) Sedimentation Basins, (3) Chemical Processing Unit, (4) Filtration Unit, (5) Water Storage Unit, and (6) High Pumping Unit. Raw water is extracted from the Al-Hilla/Al-Hashimiyah River via six iron intake pipes, each with a diameter of 50 mm, and conveyed to the Low Pumping Unit. It is then directed into six circular sedimentation basins, each with a capacity of 1,000 m^3, for preliminary settling. After sedimentation, the flow continues to the Chemical Unit, where chlorination is applied for disinfection. The clarified and disinfected water proceeds to the Filtration Unit, which comprises 32 filters distributed across four zones to ensure thorough removal of residual particulates. Following filtration, the treated water is stored in dedicated storage tanks. Distribution is then achieved through ten high-capacity pumps housed in the High Pumping Unit, with each pump strategically assigned to serve specific target districts based on demand and elevation. This plant's complex configuration and wide service coverage make it an ideal case for analysing transient flow behaviour and for conducting a sensitivity assessment of hydraulic parameters under varying operational conditions.

Figure 1: Al-Hashimiyiah water treatment plant (Google Earth)

2.2. Water Distribution Path and Hydraulic Transport System

The Al-Hashimiyah district, located in the southern region of the Babylon Governorate, is served by critical water treatment and transmission infrastructure. The distribution pathway for treated water begins at the filtration unit, where filtered water is collected in dedicated storage tanks equipped with ventilation pipes to balance internal pressure and prevent vacuum formation. From the storage tanks, water flows to the High Pumping Unit, the final stage in the treatment process [15]. This unit contains ten high-capacity pumps, each assigned to specific service areas as follows: (1) Two pumps supply the Al-Hashimiyah district; (2) Three pumps serve the Al-Qasim district; (3) Three pumps deliver water to the Al-Madhatiya district; and (4) Two pumps supply the Al-Shomali district. Each pump is connected to a discharge pipeline with a 0.25 m diameter and 500 m in length, forming the pressurised core conduits that feed the main distribution network. This study focuses on analysing transient flow behaviour, with particular emphasis on water hammer, a hydraulic phenomenon caused by abrupt changes in flow velocity, such as sudden pump stoppage or valve closure. These pressure surges can lead to significant pipeline stress, structural damage, and operational hazards if not properly understood and mitigated. The pipelines run through a semi-flat, arable terrain, offering favourable installation conditions with limited elevation-induced pressure variations [4]. This stable topography allows for a clearer assessment of pressure transients without significant interference from gravitational head fluctuations. Ultimately, this section provides valuable insights into the pipeline system's vulnerability to hydraulic transients and informs the design of effective surge protection strategies to enhance the operational reliability and safety of the Al-Hashimiyah water distribution network.

2.3. Estimation of Water Demand

The Al-Hashimiyah Water Treatment Plant plays a vital role in supplying potable water to the southern districts of Babylon Governorate, specifically Al-Hashimiyah, Al-Qasim, Al-Tali'ah, and Al-Shomali. As of the base year 2025, the plant serves an estimated 250,000 residents. In anticipation of future demographic changes, an accurate estimate of water demand through 2050 is essential for infrastructure planning, including treatment capacity, pipeline sizing, and operational scheduling. To project future population growth, demographic data were obtained from the Statistics Division of Babylon Governorate. Four standard forecasting models were evaluated: Arithmetic (Linear), Geometric, Exponential, and Logistic. Given the historically stable and predictable population growth in the region, the Arithmetic (Linear) Model was selected as the most appropriate. The Arithmetic Model assumes a constant annual increase in population and is defined by the following equation:

$$r = \frac{P_t - P_0}{P_0} \quad (1)$$

Where, r = population growth rate (%); P_0 = initial population at the base year; and P_t = projected population at year t. Assuming a fixed annual increase of 5,000 inhabitants, the population is expected to reach 375,000 by the year 2050, as illustrated in Table 1. Using the Iraqi Ministry of Planning's standard per capita water consumption rate of 300 litres/day, the projected domestic water demand for 2050 is calculated as:

$$375{,}000 \times 300 = 112{,}500{,}000 \text{ liters/day} = 1.30 \text{m}^3/\text{sec} \quad (2)$$

In addition to domestic consumption, the total water requirement must account for agricultural use and public services. Taking these into consideration, the maximum total discharge demand is estimated at approximately 1.65 m³/s. The current design discharge capacity of the plant is 6,000 m³/h, equivalent to 1.67 m³/s, which is sufficient to meet both present and near-future demands. However, by 2050, this margin is expected to narrow, emphasising the need for capacity upgrades and network optimisation to ensure sustained service delivery across the expanding service area. This demand projection provides a foundation for strategic water resource planning, system expansion, and resilience enhancement of the Al-Hashimiyah water supply network.

Table 1: Projected population growth in the Al-Hashimiyah service area (2025-2050) using the arithmetic growth model

Year	Time (t)	Projected Population (Pt) [capita]	Year	Time (t)	Projected Population (Pt) [capita]
2025	0	250,000	2038	13	315,000
2026	1	255,000	2039	14	320,000
2027	2	260,000	2040	15	325,000
2028	3	265,000	2041	16	330,000
2029	4	270,000	2042	17	335,000
2030	5	275,000	2043	18	340,000
2031	6	280,000	2044	19	345,000
2032	7	285,000	2045	20	350,000
2033	8	290,000	2046	21	355,000
2034	9	295,000	2047	22	360,000
2035	10	300,000	2048	23	365,000
2036	11	305,000	2049	24	370,000
2037	12	310,000	2050	25	375,000

2.4. Hydraulic and Pipeline Design Parameters

The total length of each distribution pipeline extending from the High Pumping Unit to its designated service district is approximately 500 meters. These pipelines convey treated water under pressure to four major districts: Al-Hashimiyah, Al-Qasim, Al-Madhatiya, and Al-Shomali. The required discharge rates for each district were determined based on the current population and projected water demand [16]. For instance, the Al-Hashimiyah district is served by two pumps, each delivering 1,000 m³/h. The Al-Qasim district uses three pumps: two provide 1,000 m³/h each, and the third delivers 400 m³/h. Similarly, Al-Madhatiya operates three pumps, each with a capacity of 1,000 m³/h. The Al-Shomali district is supported by two pumps, each rated at 700 m³/h. These discharge values reflect the distribution requirements for domestic use across the serviced areas. Based on these Figures, the maximum discharge required per pump under current demand conditions is approximately 1,000 m³/h, equivalent to 0.278 m³/s. This capacity ensures the system can meet peak domestic water demand without compromising performance or pressure stability. The uniformity in pump discharge rates also simplifies system balancing and operational control. To support this system, the pipeline network will use unplasticized polyvinyl chloride (PVC-U) pipes, selected for their strength, durability, and corrosion resistance. These pipes conform to DIN 8062 (2009) and are widely recognised for use in pressurised water transmission. Each pipe has an internal diameter of 0.25 meters and a wall thickness of 0.01 meters, suitable for high-flow conditions. At an operating temperature of 20°C, and assuming a design life of 25 years with a safety factor of 2, the allowable working pressure head for these pipes is 7 bars, equivalent to 70 meters of head. These design parameters are critical not only for routine operation but also for assessing the system's behaviour under transient conditions, such as water hammer. The selected pipe materials and dimensions ensure hydraulic efficiency, structural integrity, and longevity, making them suitable for the current and projected operational demands of the Al-Hashimiyah Water Treatment Plant network.

3. Numerical Model Formulation

The Method of Characteristics (MOC) is widely regarded as the most effective approach for simulating water hammer, thanks to its straightforward application and ability to accurately model transient flow in long, pressurised pipelines. Typically applied on a fixed spatial grid, MOC benefits from second-order schemes, which offer improved accuracy over first-order methods [37]. Two main numerical schemes, explicit and implicit, are commonly used in transient flow modelling. The explicit method offers simplicity, fast computation, and efficient handling of boundary conditions, making it ideal for long, constant-diameter pipelines. However, it is less accurate in systems with short pipes, variable cross-sections, or low wave speeds due to spatial-step constraints. In contrast, the implicit method is unconditionally stable. It allows independent control of time and space steps, making it better suited for modelling open channels or short, complex pipelines, despite its higher computational demands and more difficult boundary condition management [38]. In water treatment facilities, where most pipes are long and prismatic, the MOC is highly effective. However, challenges arise when modelling components such as draft tubes or surge tanks, which

often involve short or non-prismatic ducts. Simplifying such components with equivalent pipes can distort flow inertia and reduce model accuracy [25]. Furthermore, accurate modelling of surge tanks, critical for mitigating water hammer during sudden flow changes, requires consideration of water inertia, especially in high-head systems or where tanks are connected through narrow conduits. To overcome these limitations, this study adopts a hybrid modelling strategy that combines both explicit and implicit numerical schemes. The MOC is applied to long, uniform pipelines. At the same time, the Method of Implicit (MOI) is employed for sections involving variable cross-sections, short pipelines, or free-surface boundaries, where explicit methods alone are insufficient [9]. This integrated approach ensures greater accuracy, flexibility, and stability in simulating the complex transient behaviour of the Al-Hashimiyah water treatment system. The continuity and momentum equations governing transient flow in a variable-area duct. Both explicit (MOC) and implicit (Preissmann four-point finite difference) methods are applied to solve these water hammer equations. To evaluate the transient behaviour in the Al-Hashimiyah pipeline system, a hybrid computational approach combining MOC-MOI was developed. This model accurately simulates pressure surges and unsteady flow conditions caused by rapid operational changes, such as valve closures or pump failures [17]. The continuity and momentum equations governing transient flow in a variable-area duct are expressed as follows:

$$V\frac{\partial H}{\partial x}+\frac{\partial H}{\partial t}+\frac{a^2}{g}\frac{\partial V}{\partial x}+\frac{a^2 V}{gA}\frac{\partial A}{\partial x}-\sin\beta.V=0 \quad (3)$$

$$g\frac{\partial H}{\partial x}+V\frac{\partial V}{\partial x}+\frac{\partial V}{\partial t}+\frac{f\,V\,|V|}{2D}=0 \quad (4)$$

Where x = distance; t = time; V = mean velocity; H = pressure head; a = wave speed; A = cross-sectional area; β = pipe slope; g = gravitational acceleration; f = Darcy-Weisbach friction factor; and D = inner diameter of the pipe. Applying the Preissmann scheme to Equations. (1) and (2), the discrete control equations are derived in incremental form:

$$A_1\cdot\Delta H_{i+1}+B_1\cdot\Delta Q_{i+1}=C_1\cdot\Delta H_i+D_1\cdot\Delta Q_i+F_1 \quad (5)$$

$$A_2\cdot\Delta H_{i+1}+B_2\cdot\Delta Q_{i+1}=C_2\cdot\Delta H_i+D_2\cdot\Delta Q_i+F_2 \quad (6)$$

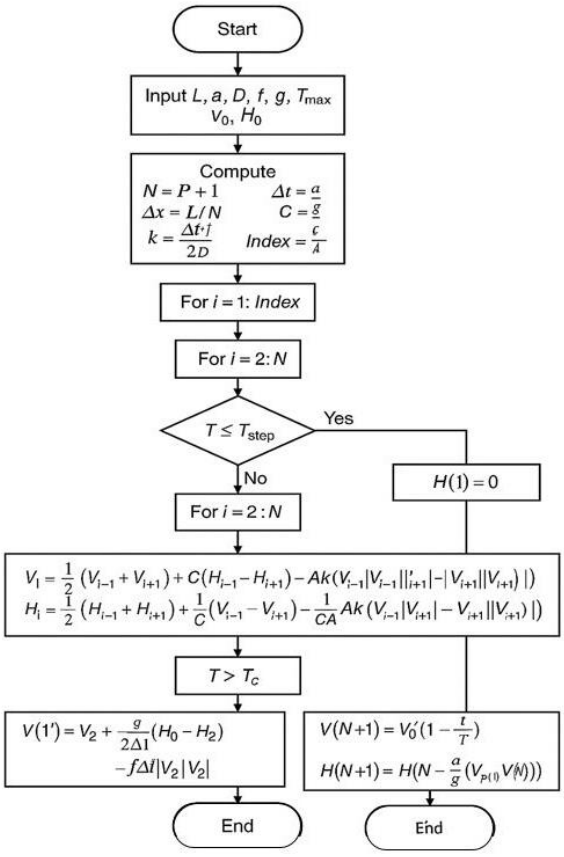

Figure 2: Flowchart of the proposed hybrid MOC-MOI model

Here, ΔH and ΔQ are the unknown increments in pressure head and discharge between time steps, and the coefficients. $A_1, B_1, \cdots, F_2$ are calculated from previous time step values and known geometry. Since Eqs (3) and (4) involve four unknowns per mesh node, the system remains open without boundary conditions. Therefore, two boundary conditions are necessary for the first and last nodes, forming a closed linear system of $2n$ equations with a bandwidth of 4 for n nodes [7]. As illustrated in Figure 2, the MOC transforms the governing partial differential equations (PDEs) into ordinary differential equations (ODEs) along characteristic lines [19]. This enables efficient, stable numerical integration of the flow behaviour along the pipeline. For simplified prismatic pipes, the model focuses on discharge and pressure head as the primary variables. The Preissmann implicit finite difference scheme is also employed for discretisation, providing unconditionally stable results and second-order accuracy via a temporal weighting factor. This scheme supports the numerical resolution of flow variables over space and time. The pipeline network is modelled using incremental forms of continuity and momentum equations. These equations are solved at each grid point at discrete time steps, accounting for changes in pressure head and discharge. The model integrates geometry, material properties, and flow dynamics while allowing flexibility in the input parameters. Boundary conditions are a critical component of the model. Boundary equations for implicit pipes at the turbine inlet and outlet:

$$Q_p = C_p - B_p \cdot H_p \tag{7}$$

$$Q_p = C_M + B_M \cdot H_s \tag{8}$$

Where Q_p is the turbine discharge, H_p is the inlet pressure head, and H_s is the outlet pressure head. Turbine unit parameter equations:

$$Q_p = Q_1^0 D_1^2 \sqrt{(H_p - H_s) + \Delta H} \tag{9}$$

$$n_1^0 = \frac{nD_1}{\sqrt{(H_p - H_s) + \Delta H}} \tag{10}$$

$$M_t = M_1^0 D_1^3 (H_p - H_s + \Delta H) \tag{11}$$

Where Q_1^0, n_1^0, and M_1^0 represent the unit discharge, unit speed, and unit torque, respectively; D_1 is the turbine diameter, and ΔH accounts for the velocity head difference between the spiral case outlet and draft tube inlet:

$$\Delta H = \left(\frac{\alpha P}{2gA_P^2} - \frac{\alpha S}{2gA_S^2}\right) Q_P^2 \tag{12}$$

With αP, αS being the kinetic energy correction factors, and A_P, A_S the respective cross-sectional areas. Turbine characteristic curves:

$$Q_1^0 = f1(n_1^0, y) \tag{13}$$

$$M_1^0 = f2(n_1^0, y) \tag{14}$$

Where y denotes the guide vane opening.

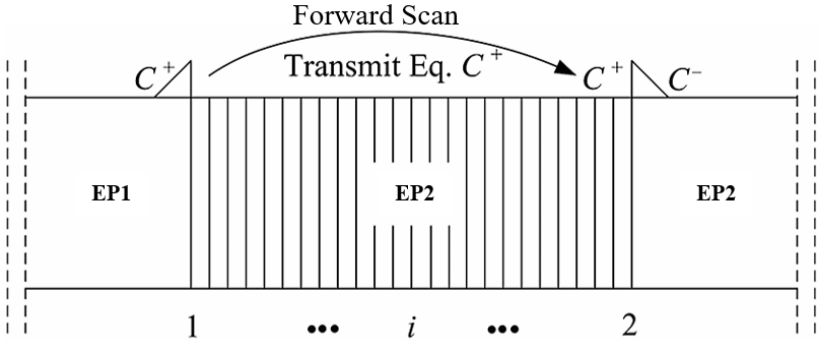

Figure 3: Coupling boundary conditions for pipes

Figure 3 illustrates boundary nodes, such as those where pipelines connect to a turbine or surge tank, are governed by equations that incorporate flow continuity, energy balance, and head losses. At these interfaces, the model couples upstream and downstream behaviours and accurately simulates interactions between system components. Lastly, the wave propagation speed is calculated based on fluid and pipe material properties, including elasticity and boundary constraints. Larock et al. [1] showed that the wave's velocity equation can be traditionally written in the general form:

$$a = \frac{\sqrt{K/\rho}}{\sqrt{1+\frac{KD}{Ee}(C)}} \quad (15)$$

Where (K) is the bulk modulus of elasticity of the fluid, (ρ) is the bulk modulus of density of the fluid, (D) is the inner diameter of the pipe, (e) is the thickness of the pipe, (E) is the modulus of elasticity (Young modulus) of the pipe material, and (C) is a coefficient that accounts for the pipe support conditions [2]. The surge tank is modelled using the MOI to track the water surface elevation over time. Its coupling with upstream and downstream pipes is governed by continuity and energy equations, ensuring consistent system behaviour during rapid transients [3]. To simulate turbine operation under transient conditions, the model includes unit discharge, speed, and torque. Guide vane positions are also considered using a time-based function that captures changes during load rejections. Additionally, the response of electric generators is modelled to account for variations in rotational speed.

4. Results and Discussion

4.1. Model Verification

The verification was performed in MATLAB using several published datasets to assess the accuracy of the current proposed hybrid MOC-MOI. The verification of the MOC-MOI model was based on a study by Jalut and Rasheed [27], which analysed the hydraulic transients in a proposed water transmission pipeline conveying water from the Diyala River to Mandali city in eastern Iraq. The total length of the pipeline is approximately 54 kilometres, extending from Five Bridges to Wadi Abi-Naft, passing through the village of Clans Neda. The system is designed to deliver a discharge of 3.5 m³/s to meet the domestic water needs. The transient analysis begins with a steady-state pressure head condition, ensuring the pressure does not exceed the maximum allowable working head of 70 meters. To sustain the hydraulic head and maintain flow continuity, three pumping stations are strategically placed: the first at the beginning of the line, the second at 22,200 meters, and the third at 39,100 meters. The remaining distance to the water treatment plant is 15,000 meters. The final pressure head at the pipeline outlet is maintained at 25 meters, providing sufficient pressure for water treatment and distribution [26].

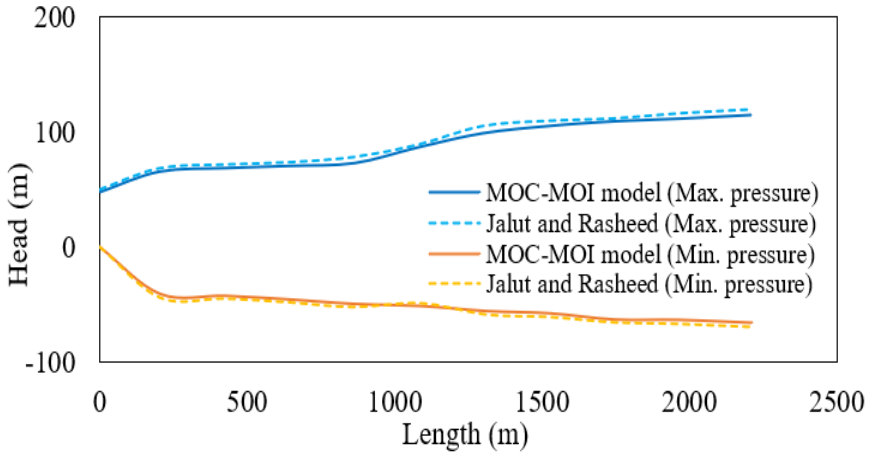

Figure 4: Comparison of maximum pressure head along the first stage pipeline under pump power failure (MOC-MOI vs Jalut and Rasheed [27] model)

Figures 4, 5, and 6 illustrate the verification of the developed MOC-MOI model against the results presented by Jalut and Rasheed [27] for transient conditions resulting from pump power failure. The comparison focuses on the maximum and minimum pressure heads for the three stages along the pipeline.

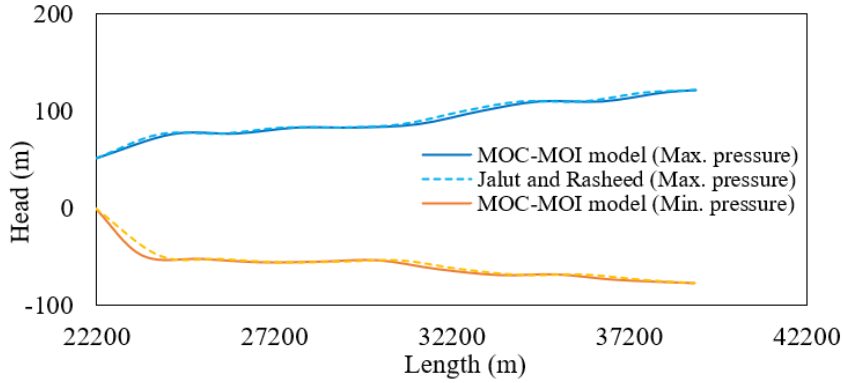

Figure 5: Comparison of minimum pressure head along the second stage pipeline under pump power failure (MOC-MOI vs Jalut and Rasheed [27] model)

The data show close agreement between the two models across the evaluated domain, with only minor variations. For example, at approximately 202 m from the pumping station, the maximum pressure calculated by the MOC-MOI model is 65.95 m, compared to 68.65 m in the Jalut and Rasheed [27] model. Similarly, the minimum pressures at this location are -40.59 m and -43.78 m for the MOC-MOI.

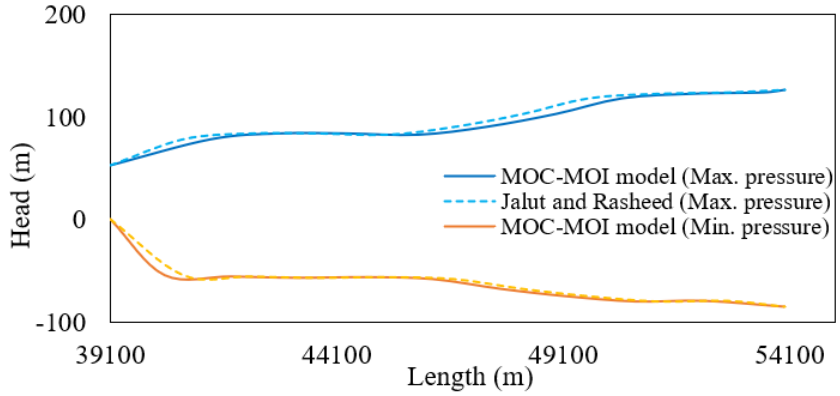

Figure 6: Comparison of minimum pressure head along the third stage pipeline under pump power failure (MOC-MOI vs Jalut and Rasheed [27] model)

As the distance increases, the trend of agreement continues; for instance, at 2206 m, the maximum pressure head reaches 115.43 m in the MOC-MOI model versus 120.24 m in the reference model, while the minimum pressure is -65.47 m compared to -68.91 m. These results confirm the robustness and reliability of the MOC-MOI simulation in capturing transient pressure variations caused by pump failures. The slightly more conservative values from the reference model highlight the importance of considering protective measures, such as surge tanks or induced valves, to safeguard the system against vapour pressure violations and potential structural damage.

4.2. Steady-State and Transient Flow Computations

Using the topographical profile, estimated water demands, and selected pipe materials, the initial steady-state conditions for pressure head (H) and flow velocity (V) were determined. The flow velocity was calculated from the continuity equation, with discharge Q = 0.278 m^3/s and a pipe cross-sectional area A = 0.0491 m^2 (diameter = 0.25 m). This results in a velocity V of roughly 5.66 m/s. The Reynolds number, calculated from the velocity, pipe diameter, and kinematic viscosity, was approximately 1.18×10^6, indicating turbulent flow. With a relative roughness (e/D) of 0.0025, the Darcy friction factor was estimated at 0.008 from the Moody diagram. The system design incorporates minor losses from valves, including gate valves before the pumping stations (loss coefficient K=0.17) and disk-type check valves after the pumping stations (loss coefficient K=10). Using the Darcy-Weisbach equation, the frictional head loss along the 500-meter pipe segments was calculated to be approximately 5.24 meters. Total head requirements, including friction and minor losses, were verified to remain within the allowable pressure head limit of 70 meters. To maintain adequate pressure and flow, the system is equipped with four pumping stations spaced along the pipeline segments.

These stations are strategically located to serve the respective districts effectively. The calculations also accounted for additional losses due to pipe fittings, bends, and safety margins. The steady-state values of head and velocity thus serve as initial conditions for subsequent transient flow analysis. The wave velocity (a) was computed using parameters such as the bulk modulus of elasticity of water ($K=2.15\times10^9$ Pa), water density ($\rho=1000$ kg/m^3), Young's modulus for iron ($E=200\times10^9$ Pa), Poisson's ratio ($\mu=0.3$), pipe diameter ($D=0.25$ m), and pipe wall thickness ($e=0.01$ m). Assuming the pipe is anchored against axial movement, the coefficient $C = 1- \mu2 = 0.91$ was used, yielding a wave velocity of approximately 1314.4 m/s. Upstream and downstream boundary conditions were applied to compute the pressure head (Hp) and velocity (Vp) at the pipe ends. These values were then iteratively updated in a time-stepping loop until the simulation reached the desired final time. The pressure head at each node was recorded throughout the simulation. The analysis showed that for a water hammer to occur, the valve closure time must be less than 100 seconds; for instance, a 60-second closure triggers significant transient pressure fluctuations. The computed pressure variations along the pipeline are illustrated in Figure 7.

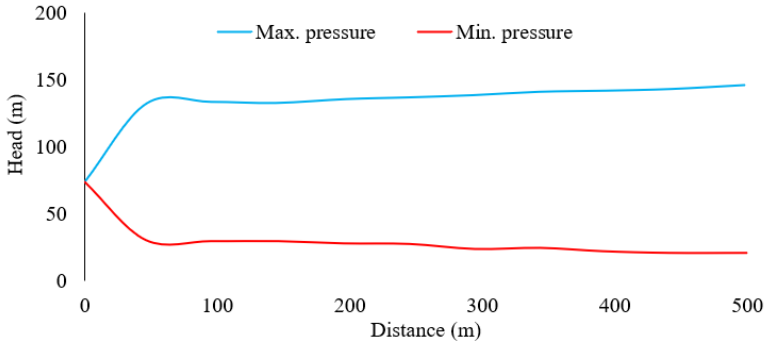

(a) Q=0.111 m^3/sec

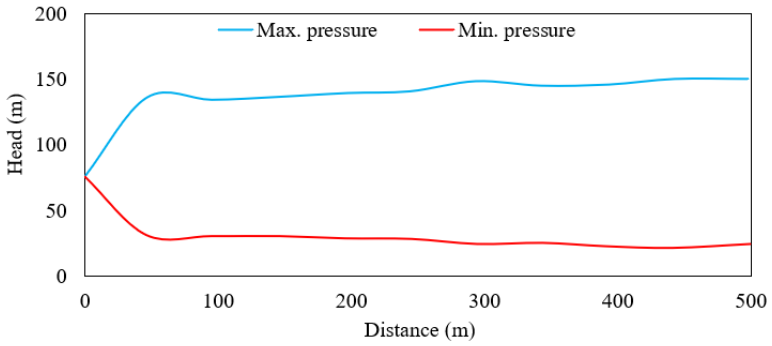

(b) Q=0.194 m^3/sec)

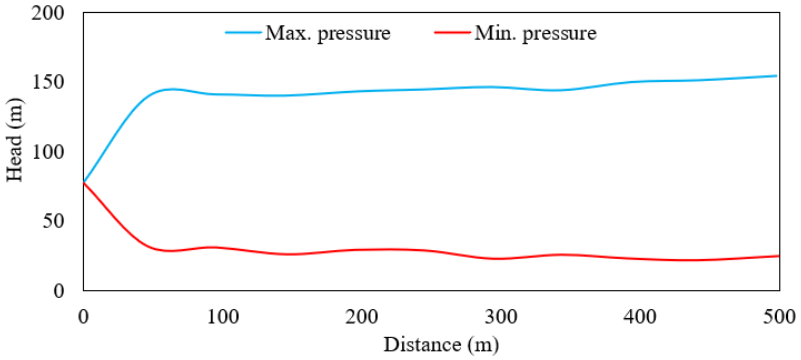

(c) Q=0.278 m^3/sec

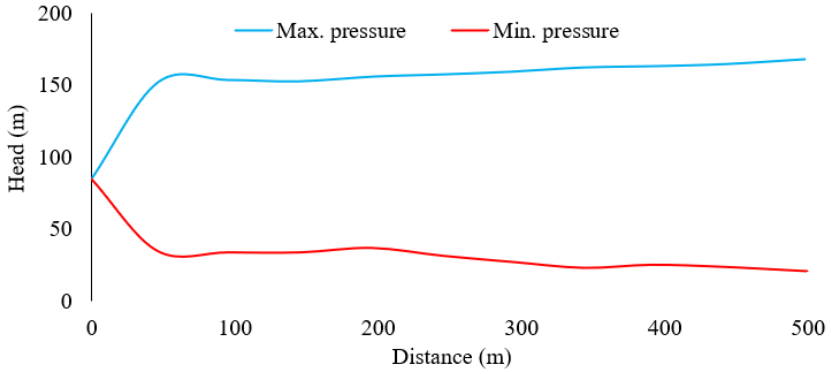

(d) Q=0.347 m^3/sec

Figure 7: Maximum and minimum pressure under different discharges and with D=0.25m, f=0.008

4.3. Hydraulic Transients Induced by Pump Power Failure

A sudden pump power failure can cause rapid changes in flow within the pipeline system. On the pump discharge side, the hydraulic grade line may drop below the pipeline elevation, causing the fluid pressure to fall to the vapour pressure and potentially leading to vapour column separation. Following pump shutdown, the water head (H) at the pumping station decreases over time, and such transient conditions can quickly lead to column separation, making predictions challenging. The consequences may include cavity collapse or extremely high pressure spikes, often triggered by the closure of check valves. Given these risks, accurately simulating hydraulic transients is crucial for system safety and reliability. The pressure fluctuations resulting from pump failure are illustrated in Figure 8. These Figures demonstrate that the maximum pressure head within the pipe increases to approximately 95.7% of the initial pressure head during the first stage, 95.9% during the second stage, and 80.7% during the third stage.

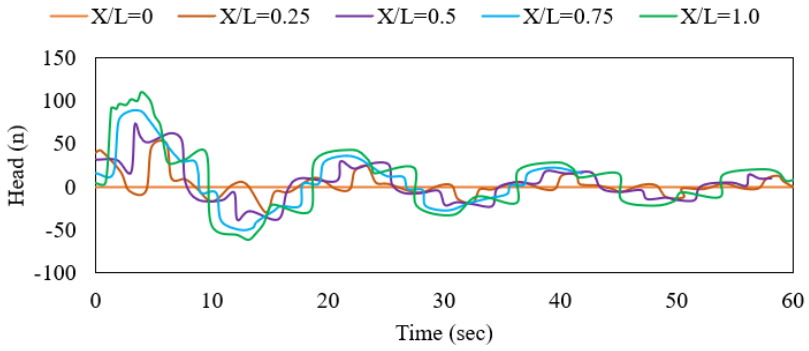

(a) Q=0.111 m^3/sec

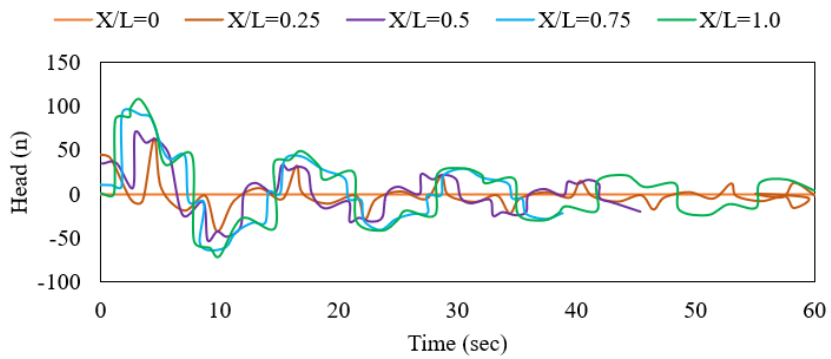

(b) Q=0.194 m^3/sec

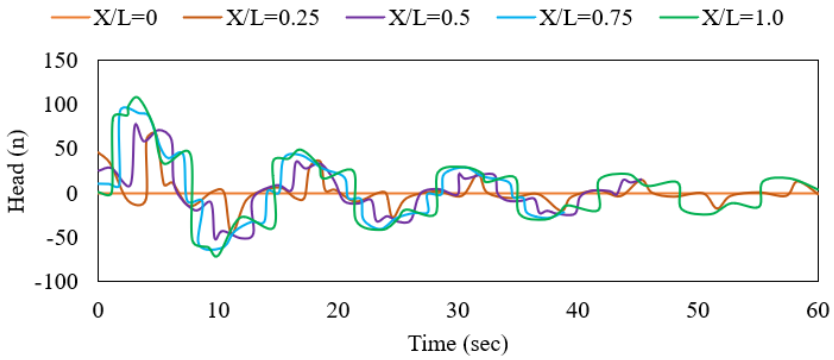

(c) Q=0.278 m^3/sec

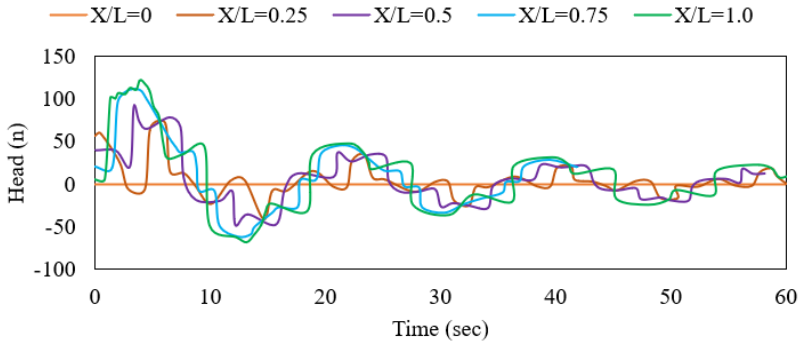

(d) Q=0.347 m^3/sec

Figure 8: Pressure fluctuations at different positions of the pipe at pump stopping under different discharges and D=0.25m, f=0.008

4.4. Mitigation of Water Hammer Due to Valve Closure

To safeguard the pipeline network supplying water from the Al-Hashimiyah Water Treatment Plant and to mitigate the harmful effects of water hammer caused by sudden valve closures or pump stoppages, the installation of a surge tank is highly recommended. Water hammer is a transient hydraulic phenomenon characterised by abrupt pressure fluctuations that can lead to pipe rupture, joint failures, and damage to system components. Surge tanks serve as an effective countermeasure by absorbing or releasing water during these transient events, thereby stabilising pressure and preserving pipeline integrity. The proposed surge tank is designed as an open cylindrical structure hydraulically connected to the pipeline. It is strategically located such that its normal water level aligns with the hydraulic grade line under steady-state flow conditions.

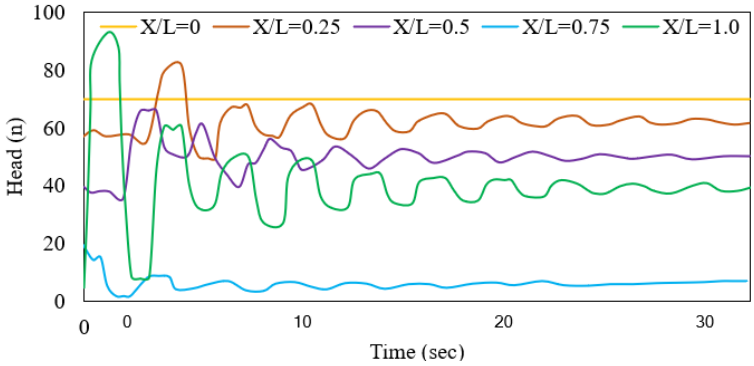

Figure 9: Pressure fluctuations at different positions of the pipe

In summary, integrating a surge tank with these specifications into the Al-Hashimiyah water supply network is a proactive approach. In the event of a pump shutdown, the tank acts as a temporary reservoir, supplying water to the system through

gravity flow. Conversely, during sudden valve closures, it receives excess flow, thus dampening pressure surges and preventing sharp spikes. For the Al-Hashimiyah system, the surge tank is sized based on a peak flow rate of 0.347 m^3/sec. With a diameter of 12 meters, the tank has a cross-sectional area of approximately 113 m^2. Transient hydraulic modelling suggests a tank height of 15 meters, providing a total storage volume of approximately 1,700 m^3. This volume is adequate to absorb pressure surges and maintain system stability during transient events. The surge tank will be installed roughly 70 meters downstream of the first pumping station. Its primary function is to control pressure fluctuations, preventing both high-pressure shocks and low-pressure vacuum conditions. This design ensures that the maximum pressure remains below the pipeline's safe working limit, particularly important for iron pipes, and helps avert cavitation risks that could cause pipe collapse—a vital measure to enhance system resilience and protect infrastructure. Hydraulic analysis confirms that the tank effectively limits transient pressures within safe operational ranges. This is further demonstrated in Figure 9, which illustrates the tank's impact on pressure wave mitigation and system layout, and in Figure 10, which compares pressure fluctuations at the pipeline's end with and without the mitigation strategy. Results indicate that the maximum pressure head in the pipeline is reduced by 24.6% when the surge tank is employed.

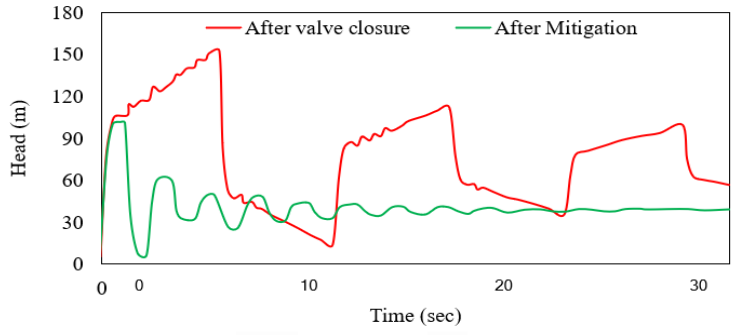

Figure 10: Comparison between protected and unprotected systems at the end of the pipe

5. Sensitivity Analysis

This section presents a sensitivity analysis of the impact of key flow properties on water hammer in the pipeline system. Specifically, the influence of pipe diameter, discharge rate, and friction factor on transient pressure surges resulting from sudden valve closures is investigated.

5.1. Sensitivity Analysis for Different Pipe Diameters

The first case focuses on how varying pipe diameters affect transient flow behaviour, with particular attention to the magnitude of pressure surges. All other parameters, including flow rate, wave velocity, friction factor, and material properties, are held constant to isolate the effects of diameter changes. For this analysis, several constants and assumptions are applied to ensure consistency. The flow rate is fixed at $Q = 0.278$ m^3/s, the pipeline length at $L = 500$ m, and the Darcy-Weisbach friction factor at $f = 0.008$. The previously calculated wave velocity is taken as $a = 1314.4$ m/s. Water density is assumed to be $\rho = 1000$ kg/m^3, representing standard conditions. Pipe thickness is adjusted proportionally with diameter to maintain structural integrity under internal pressure. The initial pressure head is set at $H = 50$ m, providing realistic initial conditions for transient pressure wave simulation (Table 2).

Table 2: Summary of flow velocity and maximum surge pressure for various pipe diameters

Pipe Diameter (m)	Cross-Sectional Area (m^2)	Velocity (m/s)	Max Surge Pressure (m)
0.2	0.0314	8.85	191.21
0.25	0.0491	5.66	164.15
0.3	0.0707	3.93	139.37
0.35	0.0962	2.89	122.32

Four pipe diameters are evaluated: 0.20 m, 0.25 m (baseline), 0.30 m, and 0.35 m. This range allows comparison of the hydraulic effects of size variation on head losses, flow velocity, and surge pressures within the system. The analysis results reveal a clear inverse correlation between pipe diameter and both flow velocity and maximum surge pressure. At the smallest diameter of 0.20 m (cross-sectional Area = 0.0314 m^2), the flow velocity reaches 8.85 m/s, producing a peak surge pressure of 191.21 m. Increasing the diameter to the baseline 0.25 m (Area = 0.0491 m^2) lowers the velocity to 5.66 m/s and reduces the surge pressure to 164.15 m. Further diameter increases to 0.30 m (Area = 0.0707 m^2) and 0.35 m (Area = 0.0962 m^2) decrease the velocity to

3.93 m/s and 2.89 m/s, respectively, with corresponding surge pressures dropping to 139.37 m and 122.32 m. These findings demonstrate that larger pipe diameters significantly diminish pressure surges, thereby reducing the risk and severity of hydraulic shock within the system.

The graph in Figure 11, which illustrates Maximum Surge Pressure against Pipe Diameter, clearly demonstrates an inverse relationship between the two variables. As the pipe diameter increases from 0.2 m to 0.35 m, the maximum surge pressure decreases significantly from 191.21 m to 122.32 m. This trend can be explained by fluid-dynamics principles governing transient flow (water hammer) in pipelines. Smaller diameter pipes generally experience higher surge pressures due to the restricted flow area, which causes greater velocity changes and thus larger pressure spikes when sudden flow changes occur (such as rapid valve closure or pump shutdown).

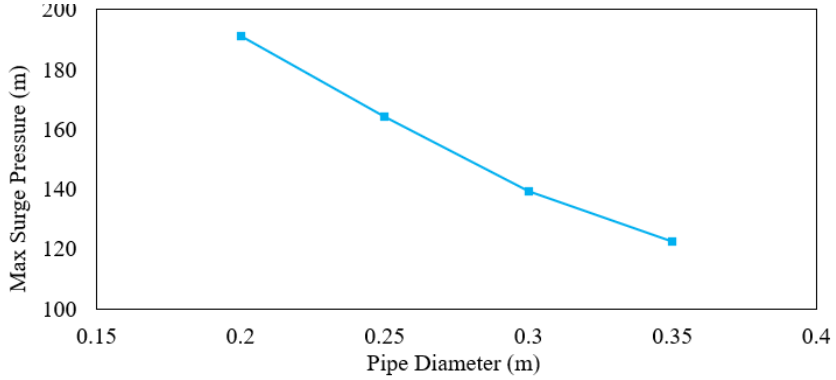

Figure 11: Variation of maximum surge pressure with pipe diameter

5.2. Sensitivity Analysis for Different Discharge Values

The second sensitivity analysis focuses on the effect of varying discharge rates (flow rates) on the pipeline's transient hydraulic response, particularly surge pressures induced by sudden valve closures. To isolate the influence of discharge, other key parameters, including pipe diameter, friction factor, wave velocity, and fluid properties, were kept constant throughout the analysis. In this study, the pipe diameter was fixed at 0.25 m, corresponding to a cross-sectional area of 0.0491 m². The wave velocity was maintained at 1314.4 m/s, the Darcy-Weisbach friction factor was set at 0.008, and water density was assumed to be 1000 kg/m³. The initial pressure head was held constant at 50 m to ensure consistency across discharge scenarios. Four discharge rates were considered to represent a spectrum of operating conditions: 0.111 m³/s (low flow), 0.194 m³/s (moderate flow), 0.278 m³/s (baseline), and 0.347 m³/s (high flow). The corresponding results are displayed in Table 3. The findings reveal a direct proportionality between discharge, flow velocity, and maximum surge pressure. At the lowest discharge of 0.111 m³/s, the flow velocity was 2.26 m/s with a surge pressure of 65.56 m. Increasing the flow to 0.194 m³/s resulted in a velocity of 3.95 m/s and a surge pressure of 114.55 m. The baseline flow of 0.278 m³/s produced a velocity of 5.66 m/s and a surge pressure of 164.15 m. The highest flow of 0.347 m³/s generated the most significant transient response, with a velocity of 7.07 m/s and a maximum surge pressure reaching 205.13 m. These results clearly indicate that as the discharge rate increases, so does the risk of damaging pressure surges in the pipeline. This is due to the higher kinetic energy associated with greater flow rates, which intensifies transient pressure spikes during abrupt flow changes.

Table 3: Summary of flow velocity and maximum surge pressure for various discharge values (D = 0.25 m, f = 0.008, a = 1314.4 m/s)

Discharge (m³/s)	Velocity (m/s)	Max Surge Pressure (m)
0.111	2.26	65.56
0.194	3.95	114.55
0.278	5.66	164.15
0.347	7.07	205.13

Figure 12 presents the relationship between discharge rate and the corresponding maximum surge pressure observed in the pipeline system during sudden valve closure. The graph clearly illustrates a strong, positive, and nonlinear correlation between these two parameters. As discharge increases, the resulting surge pressure rises significantly, reflecting the direct impact of flow rate on transient hydraulic responses. These results emphasise the critical role of discharge in determining the severity of hydraulic transients. Systems operating at high discharge rates are significantly more vulnerable to water hammer, which can

cause structural damage, pipeline rupture, or failure of valves and fittings. Therefore, engineers must account for this relationship when designing or upgrading pipeline systems. Appropriate mitigation measures, such as surge tanks, pressure relief valves, or gradual valve-closure strategies, should be considered for high-flow applications to protect infrastructure and ensure operational safety.

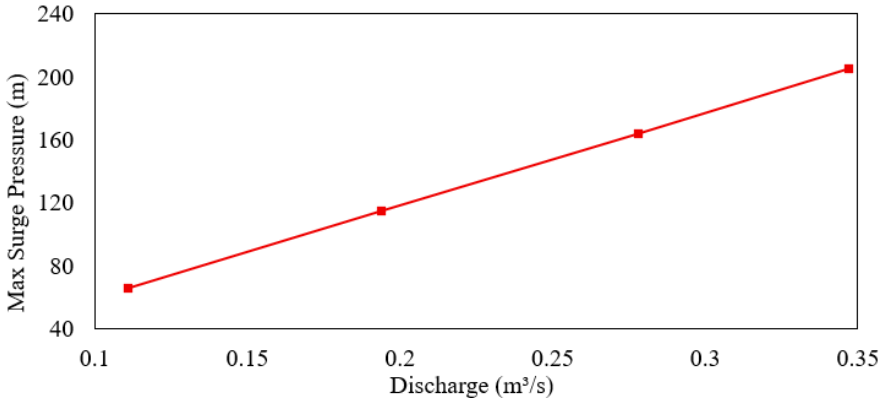

Figure 12: Variation of maximum surge pressure with discharge

5.3. Sensitivity Analysis for Different Friction Factors

The third sensitivity analysis examines how variations in the Darcy-Weisbach friction factor affect the transient hydraulic response of the pipeline system, with particular focus on surge pressures generated by sudden valve closures. The friction factor represents the internal flow resistance within the pipe and is influenced by factors such as pipe material, surface roughness, ageing, and corrosion. Understanding its impact is vital for assessing the system's ability to dampen pressure surges and maintain safe operation under transient conditions. In this study, the discharge was fixed at the baseline value of 0.278 m^3/s, with a pipe diameter of 0.25 m and a corresponding cross-sectional area of 0.0491 m^2. The wave velocity was held constant at 1314.4 m/s, water density at 1000 kg/m^3, and the initial pressure head at 50 m. These consistent parameters allowed for a controlled evaluation of the friction factor's influence on surge magnitude. Four friction factor values were selected to cover a realistic range encountered in practice: 0.003, representing very smooth new steel or plastic pipes; 0.006, typical of clean, smooth pipes; 0.008, the baseline case; and 0.012, reflecting roughened or aged pipes affected by corrosion or scaling. The results, summarised in Table 4, demonstrate a clear damping effect from increasing friction. Specifically, the lowest friction factor of 0.003 produced the highest surge pressure of about 187.40 m due to minimal energy loss. Increasing the friction to 0.006 reduced the surge pressure to 175.20 m. At the baseline friction of 0.008, the maximum surge pressure decreased further to 164.15 m. The highest friction factor, 0.012, significantly lowered the surge pressure to 149.80 m, indicating substantial damping. These findings highlight the crucial role of pipe roughness in mitigating water hammer. While smoother pipes promote efficient steady-state flow, they are more susceptible to higher surge pressures during transient events. Conversely, rough or aged pipes provide additional flow resistance, naturally reducing pressure spikes. Hence, accurately estimating the friction factor, especially as pipelines age, is essential for reliable surge pressure prediction and the design of effective protective measures.

Table 4: Effect of friction factor on maximum surge pressure (Q = 0.278 m^3/s, D = 0.25 m, a = 1314.4 m/s)

Friction Factor (f)	Flow Velocity (m/s)	Max Surge Pressure (m)
0.003	5.66	187.4
0.006	5.66	175.2
0.008 (baseline)	5.66	164.15
0.012	5.66	149.8

Figure 13 presents the relationship between the Darcy-Weisbach friction factor and the resulting maximum surge pressure in an unprotected pipeline system under sudden valve closure. The graph clearly illustrates an inverse relationship: as the friction factor increases, the maximum surge pressure decreases. This trend highlights the important role of pipe wall roughness in attenuating pressure waves. At a low friction factor of f=0.003, which corresponds to a very smooth internal pipe surface (e.g., new steel or plastic), the surge pressure reaches a peak of 187.40 m. In this case, minimal internal resistance allows the pressure wave to propagate with little energy loss, resulting in a more severe hydraulic response. As the friction factor increases from f=0.006 to f=0.008, and ultimately to f=0.012, the pressure surges progressively reduce to 175.20 m, 164.15 m (baseline), and 149.80 m, respectively. This decline reflects greater energy dissipation in rougher pipes, which absorb more of the wave's

kinetic energy and dampen its amplitude. The nonlinear nature of the curve also suggests that friction's effectiveness in reducing surge pressure is greater at lower values and tapers off as friction increases. This is particularly important in design scenarios where minor increases in roughness, due to pipe ageing, scaling, or material choice, can meaningfully reduce surge pressures and improve system resilience. Also, Figure 13 reinforces the need for accurate estimation of pipe friction factors during both the design and operational phases. Understanding the damping behaviour introduced by internal roughness is essential for predicting system performance under transient conditions and for selecting appropriate surge protection strategies when required.

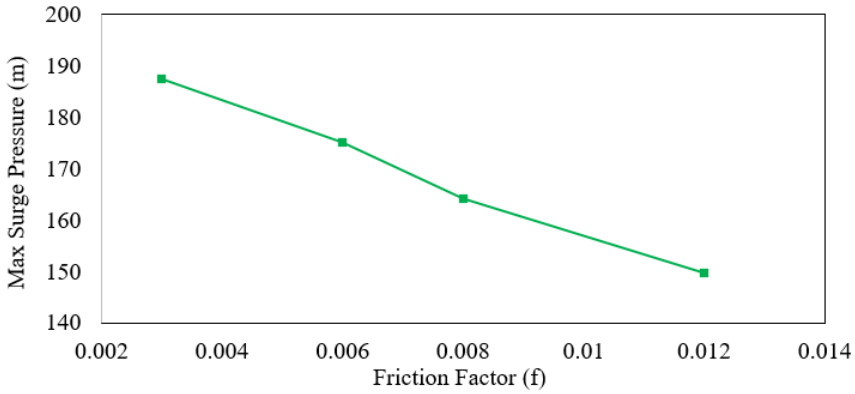

Figure 13: Variation of maximum surge pressure with friction factor (f)

6. Conclusion

A comprehensive investigation of steady and unsteady flow conditions in the Al-Hashimiyah water transmission system has led to several important conclusions. The steady-state analysis indicated a flow velocity of 5.66 m/s, with a Reynolds number of approximately 1.18×10^6 and a Darcy-Weisbach friction factor of 0.008. Under these conditions, the total head losses were maintained below the allowable design limit of 70 meters, confirming the adequacy of the system for current demands. The hybrid numerical model combining the Method of Characteristics (MOC) and Method of Integration (MOI) successfully simulated transient flow phenomena, demonstrating reliability and accuracy in predicting pressure surges and fluctuations throughout the pipeline network. Rapid valve closures were identified as a critical source of significant pressure surges, particularly in downstream sections, with peak pressures approaching critical limits at high flow rates of up to 0.347 m^3/s. Similarly, sudden pump power failure caused sharp pressure drops and negative pressures, increasing the likelihood of cavitation and column separation within the pipeline. To mitigate these effects, the installation of a surge tank measuring 12 meters in diameter, 15 meters in height, and providing approximately 1,700 cubic meters of storage, 70 meters downstream of the first pumping station, was found to reduce peak pressure surges by nearly 25% effectively. Sensitivity analyses revealed that increasing the pipe diameter from 0.20 m to 0.35 m correspondingly lowered the maximum surge pressure from 191.21 m to 122.32 m. Surge pressures increased nonlinearly with discharge, ranging from 65.56 m at a low flow of 0.111 m^3/s to 205.13 m at a high flow of 0.347 m^3/s. Additionally, higher friction factors, ranging from 0.003 to 0.012, reduced peak surge pressure from 187.40 m to 149.80 m, highlighting the significant damping effect of pipe roughness. Overall, the MOC-MOI hybrid approach proved to be an effective and versatile modelling tool capable of capturing the essential dynamics of hydraulic transients in the Al-Hashimiyah water transmission system. Its flexibility in parameter adjustment and robust predictive capabilities make it highly valuable for design optimisation, risk assessment, and the development of protective strategies for similar water supply infrastructures.

Acknowledgement: The authors sincerely acknowledge the academic support and research facilities provided by Al-Qasim Green University, University of Kufa, and University of Warith Al-Anbiyaa. Their cooperation and scholarly environment greatly contributed to the successful completion of this work.

Data Availability Statement: The datasets used in this study can be obtained from the corresponding author upon reasonable request.

Funding Statement: No external funding was received for the conduct or preparation of this research.

Conflicts of Interest Statement: The authors declare no competing interests, and all sources have been properly acknowledged.

Ethics and Consent Statement: The study was conducted in compliance with ethical standards, with informed consent obtained and participant confidentiality strictly maintained.

References

1. B. E. Larock, R. W. Jeppson, and G. Z. Watters, "Hydraulics of Pipeline Systems," *CRC Press*, Florida, United States of America, 1999.
2. B. S. Jung and B. Karney, "A practical overview of unsteady pipe flow modeling: From physics to numerical solutions," *Urban Water Journal*, vol. 14, no. 5, pp. 502–508, 2017.
3. C. Wang and J. D. Yang, "Water hammer simulation using explicit–implicit coupling methods," *Journal of Hydraulic Engineering*, vol. 141, no. 4, p. 04014086, 2015.
4. D. Leary, B. Theriault, A. Sommerville, and M. Nixon, "The importance of terrain analysis for pipeline planning and pipeline asset management," in *Pipelines, American Society of Civil Engineers*, Reston, Virginia, United States of America, 2018.
5. H. E. Schulz, J. G. Vasconcelos, and A. C. Patrick, "Air entrainment in pipe-filling bores and pressurization interfaces," *Journal of Hydraulic Engineering*, vol. 146, no. 2, pp. 1–32, 2020.
6. H. F. Duan, "Uncertainty analysis of transient flow modeling and transient-based leak detection in elastic water pipeline systems," *Water Resources Management*, vol. 29, no. 14, pp. 5413–5427, 2015.
7. J. He, Q. Hou, X. Yang, H. Duan, and L. Lin, "Isolated slug travelling in a voided line and impacting at an end orifice," *Physics of Fluids*, vol. 36, no. 2, pp. 1–11, 2024.
8. J. Liang, Z. Liu, Z. He, H. Liu, and Z. Shao, "Development of a novel finite element submodeling technique for fatigue reliability modeling and assessment of wind turbine blades," *Ocean Engineering*, vol. 316, no. 5, p. 119934, 2025.
9. J. Moradi, A. M. Andwari, and J. Könnö, "Numerical methods for the flow fields: A comparative review," in *Proc. Second SIMS EUROSIM Conf. on Modelling and Simulation (SIMS EUROSIM)*, Oulu, Finland, 2025.
10. J. Ye, M. Lambert, W. Zeng, and N. C. Do, "Extended method of characteristics for inverse hydraulic transient modeling using sensor data," *Journal of Hydraulic Engineering*, vol. 151, no. 4, pp. 1–28, 2025.
11. K. R. Knapp, A. N. Palazotto, and O. E. Scott-Emuakpor, "Comparison of finite element strain distribution to in situ strain field of a plastically-deformed plate," in *Proc. 58th AIAA/ASCE/AHS/ASC Structures, Structural Dynamics, and Materials Conf.*, Texas, United States of America, 2017.
12. K. Urbanowicz, H. Jing, A. Bergant, M. Stosiak, and M. Lubecki, "Progress in analytical modeling of water hammer," *Journal of Fluids Engineering*, vol. 145, no. 8, pp. 1–12, 2023.
13. L. Abdulameer, A. N. Al-Dujaili, M. S. Al-Kafaji, N. M. Al Maimuri, and K. Shemal, "Impact of outlets manifold configuration on hydraulic stability and water hammer in pumping stations," *Results in Engineering*, vol. 26, no. 6, pp. 1–12, 2025.
14. L. G. Britton and R. J. Willey, "Avoiding water hammer and other hydraulic transients," *Process Safety Progress*, vol. 43, no. 1, pp. 101–112, 2024.
15. L. L. Swatridge, R. P. Mulligan, L. Boegman, and S. Shan, "Development and performance of a high-resolution surface wave and storm surge forecast model: Application to a Large Lake," *Geoscientific Model Development*, vol. 17, no. 21, pp. 7751–7766, 2024.
16. L. Scholten, M. Maurer, and J. Lienert, "Comparing multi-criteria decision analysis and integrated assessment to support long-term water supply planning," *PLoS ONE*, vol. 12, no. 5, pp. 1–30, 2017.
17. L. Tukenova, O. Auyelbekov, S. Sapakova, B. Abduraimova, Z. Ualiyev, A. Kabdoldina, G. Turken, and A. R. Kalpebaev, "Research of the finite difference numerical method using artificial intelligence for solving problems of incompressible fluid flow in a rectangular domain with initial and boundary conditions," *Engineered Science*, vol. 34, no. 2, pp. 1–13, 2025.
18. F. Salmasi, "Sensitivity analysis for water hammer problem in pipelines," *Iranica Journal of Energy and Environment*, vol. 5, no. 2, pp. 1-8, 2014.
19. M. Assaf, "Modeling and understanding flow transients in unusual cases in water systems, PhD dissertation, *Polytechnic University of Turin*, Turin, Italy, 2024.
20. M. F. Almasooudi and S. Rahman, "An empirical evaluation of tour guide and tourism policy: The case of Babylon, Iraq," *Management*, vol. 9, no. 35, pp. 72–105, 2024.
21. M. H. Arefi, M. Ghaeini-Hessaroeyeh, and R. Memarzadeh, "Numerical modeling of water hammer in long water transmission pipeline," *Applied Water Science*, vol. 11, no. 8, pp. 1–10, 2021.
22. M. Kandil, T. A. El-Sayed, and A. M. Kamal, "Unveiling the impact of pipe materials on water hammer in pressure pipelines: An experimental and numerical study," *Scientific Reports*, vol. 14, no. 1, pp. 1–26, 2024.
23. M. Mason, "Infrastructure under pressure: Water management and state-making in southern Iraq," *Geoforum*, vol. 132, no. 4, pp. 52–61, 2022.

24. M. Sedlar and P. Abrahámek, “A numerical study on the performance of a pumping station with bell-mouth-based vertical pumps during an accidental shutdown,” *Processes*, vol. 12, no. 4, pp. 1–24, 2024.
25. P. Gupta and A. Bharat, “An integrated approach for capturing intermediate demographic changes,” *Journal of Urban Planning and Development*, vol. 148, no. 2, p. 04022018, 2022.
26. P. R. Goncalves, “A geometrically exact beam finite element for non-prismatic strip beams: The spatial case,” *International Journal of Structural Stability and Dynamics*, vol. 24, no. 12, p. 2450138, 2024.
27. Q. H. Jalut and N. J. Rasheed, “Mathematical modeling for water hammer in pipe flow,” *Journal of Engineering and Sustainable Development*, vol. 22, no. 1, pp. 95–108, 2018.
28. R. Taiwo, M. E. A. Ben Seghier, and T. Zayed, “Toward sustainable water infrastructure: The state-of-the-art for modeling the failure probability of water pipes,” *Water Resources Research*, vol. 59, no. 4, pp. 1–32, 2023.
29. S. I. Lupa, M. Gagnon, S. Muntean, and G. Abdul-Nour, “The impact of water hammer on hydraulic power units,” *Energies*, vol. 15, no. 4, pp. 1–27, 2022.
30. S. M. Negharchi and R. Shafaghat, “The numerical development of MOC for analyzing the inclined pipelines using the experimental network of Babol Noshirvani University as a case study,” *AQUA—Water Infrastructure, Ecosystems and Society*, vol. 70, no. 5, pp. 741–756, 2021.
31. S. Meniconi, B. Brunone, and M. Ferrante, “Water-hammer pressure waves interaction at cross-section changes in series in viscoelastic pipes,” *Journal of Fluids and Structures*, vol. 33, no. 3, pp. 44–58, 2024.
32. S. Toprak, B. P. Wham, E. Nacaroglu, M. Ceylan, O. Dal, and A. E. Senturk, “Impact of seismic geohazards on water supply systems and pipeline performance: Insights from the 2023 Kahramanmaras earthquakes,” *Engineering Geology*, vol. 340, no. 10, p. 107681, 2024.
33. S. Wei, S. Song, B. Shi, and J. Gong, “A novel approach integrating the method of characteristics with large time-step scheme (MOC-LTS) for efficient transient flow simulation in liquid pipelines,” *Journal of Pipeline Science and Engineering*, vol. 5, no. 1, pp. 1–12, 2025.
34. T. Ko, R. Farmani, E. Keedwell, and R. Beig Zali, “Risk-based water pipe failure prediction through machine learning and hydraulic models,” *Journal of Water Resources Planning and Management*, vol. 151, no. 9, pp. 1–47, 2025.
35. T. Peach, J. F. Cornhill, A. Nguyen, H. Riina, and Y. Ventikos, “The ‘Sphere’: A dedicated bifurcation aneurysm flow-diverter device,” *Cardiovascular Engineering and Technology*, vol. 5, no. 4, pp. 334–347, 2014.
36. V. Tjuatja, A. Keramat, B. Pan, H. F. Duan, B. Brunone, and S. Meniconi, “Transient flow modeling in viscoelastic pipes: A comprehensive review of literature and analysis,” *Physics of Fluids*, vol. 35, no. 8, pp. 1–31, 2023.
37. X. Mao, G. Wen, Y. Wang, J. Hu, X. Gan, and P. Zhong, “Development of WHED Method to study operational stability of typical transitions in a hydropower plant and a pumped storage plant,” *Energies*, vol. 18, no. 6, pp. 1–28, 2025.
38. Y. Wang, T. Wang, Y. Ran, X. Zhang, X. Guo, and S. Liu, “The water hammer characteristics of long-distance water pipelines under different water supply modes,” *Water*, vol. 16, no. 14, pp. 1–14, 2024.
39. Z. Qian, P. Wu, Z. Guo, and W. Huai, “Numerical simulation of air entrainment and suppression in pump sump,” *Science China Technological Sciences*, vol. 59, no. 12, pp. 1847–1855, 2016.